iJRASET
International Journal For Research in Applied Science and Engineering Technology



# INTERNATIONAL JOURNAL FOR RESEARCH

IN APPLIED SCIENCE & ENGINEERING TECHNOLOGY

**Volume:** 10 **Issue:** VIII **Month of publication:** August 2022

**DOI:** https://doi.org/10.22214/ijraset.2022.46206

www.ijraset.com

Call: 08813907089 | E-mail ID: ijraset@gmail.com

International Journal for Research in Applied Science & Engineering Technology (IJRASET)
*ISSN: 2321-9653; IC Value: 45.98; SJ Impact Factor: 7.538*
*Volume 10 Issue VIII August 2022- Available at www.ijraset.com*

# Determining the Optimal Surface Finish for a Titanium Alloy

Dharmveer Bairwa[1], Associate Prof. Bhasker Shrivastava[2]
[1, 2]*Yagyavalkya Institute of technology, Jaipur*

***Abstract: Presently a day, with the evolving times, the utilization of titanium composite expanding, for example, avionic business, military hardware, modern applications, many sorts of transportation framework, home machines and so on yet for the most part in clinical gadgets, for example, dental inserts, hip joint, complete knee substitution and a lot more because of its profile similarity.***

***Many of the applications needs to have a fine surface finish so to have a minimum surface roughness. In this paper the minimisation of surface roughness is done by using some statistical methods to take out the optimal conditions. Later, a CNC machine is used for finishing while applying the conditions we developed through statistical methods.***

## I. INTRODUCTION

In present time, not many metals are so exceptionally significant as Titanium in metal enterprises. In fact, only a handful of few metals today are as crucial to the metal industry as titanium. With its distinctive qualities, it has played a significant role in numerous manufacturing and industries. This is also because of using more and more resources of the earth many of them are on the brink of finishing line. To create the parts items with rising efficiency and better quality comes than be testing even with the swelled advantages of titanium compounds.

As the name gives it characteristics, titanium is an alloy and have other chemical elements also which gives it a very durable and extra strength to standout from other alloys. Also, we have seen the wheels boult of the infamous Bugatti car is also made form titanium alloy, which gives it strength all alone. The combination of titanium with others are very distinguish, the customary cycles are the key issue. Regardless of that the non-traditional interaction can machine this prevalent strength material effectively.

As it has more chemical elements than one, at higher temperature, we have observed other characteristics of tremendous strength and hardness for the same.

They are likewise lightweight. Titanium composite is utilized in airplane, clinical gadgets, space apparatus, military applications, gems, bikes, and the associating pole in very good quality games vehicles as a profoundly pushed part, as well as numerous purchaser hardware and select athletic gear.

It has additionally been used for dental and muscular inserts. Generally, titanium is joined with small amounts of aluminium and vanadium, around 6% and 4% by weight, individually.

Despite being a difficult material to process, titanium and its mixtures have many uses in the aviation, biomedical, substance, auto, and oil industries thanks to their exceptional physical and metallurgical characteristics.

Despite the methods used to turn this metal into chips, Siekman noted that "machining of titanium and its composites would continually be a problem." [1]. Ti6Al4V, which belongs to the alpha and beta alloy group and makes up more than half of all titanium alloys produced, is the most popular titanium alloy.

However, new alloys are being created in order to reduce weight.

The Ti555.3 alloy, one of the most recently created alloys, can be heat treated to high strengths and has a minimum tensile strength value exceeding 1200 MPa.

Compared to more conventional titanium alloys like Ti6Al4V, Ti555.3 has a higher tensile strength, making it a suitable material for advanced structural and landing gear applications [2].

Applications requiring strong corrosion resistance and low density, such as those in the aerospace industry, the automobile industry, the nuclear business, the chemical industry, the maritime industry, and biomechanical applications, all employ Ti6Al4V.(Implants and prostheses). Titanium and its metal matrix substances' popularity as a biomaterial in dentistry and medicine profession has been very well established on the basis of their improved physical and chemical structure, such as low module of elasticity, light weight, particularly high strength (strength to weight ratio), and magnificent rusting resistances, as shown in fig. 1.

©IJRASET: All Rights are Reserved 

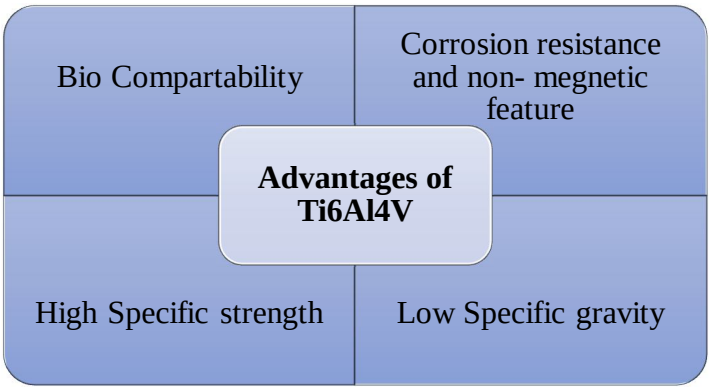



Fig. 1 Advantages of Ti-6Al-4V

## II. PRESENTATION OF THE TITANIUM ALLOYS

The titanium alloy Ti555.3, which is a member of the near-beta alloy family, has a metastable beta structure. Because of the presence of beta stabilisers like Mo, V, Fe, and Cr, etc., this different behaviour is possible.

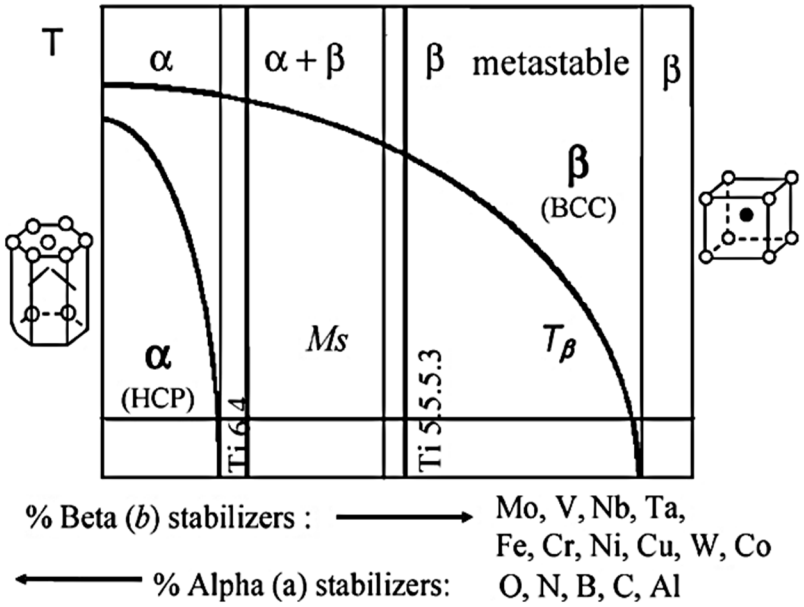



Fig. 2 Phase diagram of the titanium alloys

Ti6Al4V contains a significant amount around 80 % of the primary or residual alpha phase, whereas Ti555.3 contains around 20% of the globular residual alpha phase along with the beta-alpha Widmanstätten-transformed phase. The titanium alloys can also be classified on the bases of Al and Mo and the values of these two parameters [2].

Table 1 Chemical composition in weight percentage, Al and Mo equivalent value, and mechanical properties for the two Ti alloys

| Titanium Alloy | Chemical Composition | | | | | | | Al equiv. value (%) | Mo equiv. value (%) | Transus beta ($^{O}$C) | TYS (MPa) | UTS (MPa) | Elongation (%) | Hard.HB±5 | Tensile strength, 400 $^{O}$C (MPa) |
|---|---|---|---|---|---|---|---|---|---|---|---|---|---|---|---|
| | Al | Mo | V | Fe | Cr | Sn | Zr | | | | | | | | |
| Ti6Al4V | 6 | - | 4 | - | - | - | - | 7 | 2.5 | 995 | 900 | 1000 | 18 | 241 | 550 |
| Ti555.3 | 5 | 5 | 5 | 0.3 | 3 | - | - | 5 | 19 | 860 | 1050 | 1200 | 10 | 270 | 860 |
| Al equiv. weight value (%) = Al + Sn/3 + Zr/6 + 10 ($O^2$ + $N^2$). | | | | | | | | | | | | | | | |
| Mo equiv. weight value (%) = Mo + 2V/3 + Nb/3 + 3 (Fe + Cr). | | | | | | | | | | | | | | | |

## III. BACKGROUND

The demand on engineers to produce complex shapes with narrow tolerances is constantly growing due to the constant introduction of newer materials and the seemingly endless applications in industry. In this regard, machining of unusual materials such as titanium is critical. Titanium and its composite materials are increasingly used in commercial and industrial applications due to their excellent properties such as high temperatures, strength, a high strength-to-weight ratio, and exceptional corrosion resistance. The alloys are used in biomedical applications, transportation applications, aerospace, and a variety of other corrosive environments.

By this point, the majority of recent efforts have been developed to enhance the bone-implant interface, with the goal of increasing insert and bone repair amalgamation through physiochemical means [3]. Current findings have shown that the fracture toughness, resistance to corrosion, and biological characteristics of titanium and titanium alloys can be improved disingenuously using appropriate surface treatment methods while retaining the desirable bulk properties of the samples. Surface treatment improves the use of titanium and titanium alloys in biomedical applications [4]

Life cycle percentages for dental inserts range from 90 % - 96.5 %, whereas for orthopaedic inserts the following percentages are recorded: 98.4 % - 98.7 % at ten years for total knee prosthesis (TKP), 53 % - 90 % at five years for total elbow arthroplasty (TEA), 80 % - 94 % at fifteen years for total hip arthroplasty (THA), and 91 % at ten years for shoulder arthroplasty in patients [5], [6].

According to research, a titanium alloy with a mean surface roughness of 0.5- 1.5 m has a stronger, harder tissue reaction than one with a roughness of less than 0.5- 1.5 m [7]. However, the hard tissue response to titanium composite material surface roughness is still being debated, and there is no consistency or general approval in this area. Peptides, proteins, and growth expansion factors, in particular, have been studied on insert surfaces [8]. Furthermore, successful reactions have been demonstrated in study with real organisms. One of the most intriguing and promising approaches to achieving antimicrobial covering for titanium is the combination of inorganic metallic antibacterial agents on the titanium oxide coating [9]. Jin et al. [10] also explore the antibacterial effect of silver (Ag) and zinc (Zn) co-establishment in titanium plates.

Mechanical methods were one of the first approaches for surface deformation of titanium and its composite materials. These techniques were developed to provide titanium alloy a generic form for a variety of applications. Grinding, machining, polishing, and surface blasting are all mechanical operations that are still used in the field of biomedical sciences. These processes may produce surface roughness, which is regarded to be favourable for the creation of hard tissue cells and bio-mineralization [11]. Existing applications include ultracentrifuges and racing car components, but one of the most rapidly increasing sectors is medical, where the material is implanted in various forms into the body or utilised for products such as wheelchairs and artificial limb components. Future uses include steam turbine blading, flue gas desulphurisation plant consumer items, and a variety of maritime applications [12].

Classic machining tools for titanium and related alloys include tungsten carbide tools and high-speed steels. Because of the heat conductivity of titanium composite materials, both of these cutting tools can only be used at a slow cutting speed. When machining at faster cutting speeds, both of these cutting tools have a rather limited lifetime, hence constant cutter regrinding is required. Many of the supporting literature is already in public domain for more observations, some of which is mentioned in the paper [13]–[15].

## IV. METHODOLOGY

In contrast to standard approaches, an exclusive powerful optimization discipline has been developed based on the Taguchi improvement technique. Traditional experimental design approaches are more sophisticated and more consuming than Taguchi-based methodology. Taguchi approach employs a unique very fractionated component designs and various types of fractional designs obtained from the orthogonal array to examine the whole tentative region applicability for researchers with a small number of trails (OA). This reduces the cost of trails and time while also allowing for an improvement in the operation to be completed.

The Taguchi technique is a method for discovering the ideal control factor values to make a material or procedure noise-insensitive. Taguchi's methods are widely utilised in engineering design and may be used to a wide range of tasks such as optimization, exploratory research, risk assessment, parameterization, model prediction, and so on.

The symmetrical exhibit's lines address the different paths (combinations of trails), while the symmetrical cluster's segments address the trial boundaries to be gotten to the next level. The examination of means (ANOM) is utilized to accomplish upgraded control factors at different levels in view of the sound to commotion (S/N) proportion. The best level for deciding in the exploratory locale is the level that creates the most noteworthy worth of sound to commotion proportion.

In Taguchi boundary plan, the examination of fluctuation (ANOVA) is used to assess the overall importance of control factors and is performed on sound to commotion (S/N) to ascertain the percent (percent) commitment of all cycle boundaries.

Contingent upon the quality component to be upgraded, a few S/N proportions may be picked:

Table 2 Signal to Noise ratio observed

| Signal to Noise Ratio | Formula |
|---|---|
| Larger – the better | $-10 \times \log 10\ (sum\ (1/Y)^2/n)$ |
| Nominal – the better | $-10 \times \log 10\ (s^2)$ |
| Nominal – the better | $-10 \times \log 10\ (Ybar^2/s^2$ |
| Smaller – the better | $-10 \times \log 10\ (sum\ (Y^2/n)$ |

Where n = number of measurements in trial/row, in this case n=1, 2…, 9 and yi is the $i^{th}$ measured value in a run/row. i =1, 2……

*A. Work Materials*

We have taken two most important work materials tools, which are used in numerous experiments in the past as observed in the literature. The two main tools components are Tungsten carbide tool and High carbon steel tool.

The materials for the work and tool used are mentioned below with the chemical and physical properties:

*1) Tungsten Carbide tool*

Table 3 Chemical constituents of Tungsten carbide tool

| Elements | Cobalt (Co) | WC |
|---|---|---|
| Wt% | 6.2 | 93.8 |

Below are given the picture of tool used for the work in process.

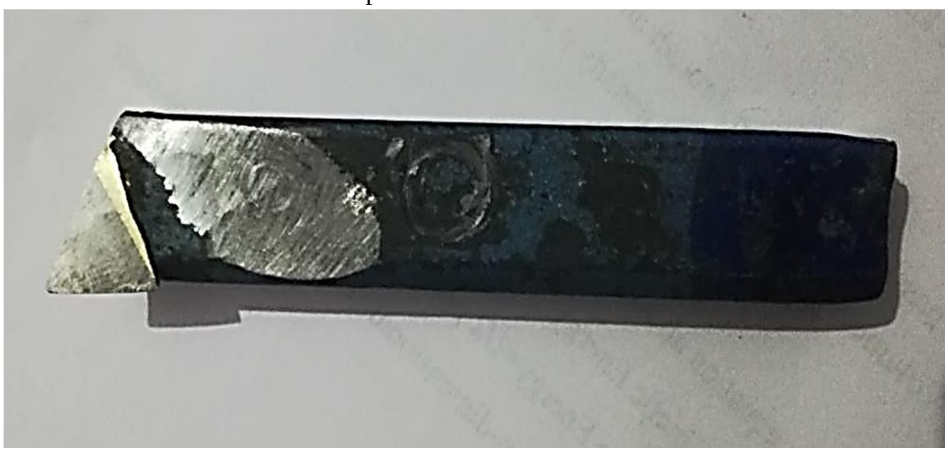


Fig.3 Tungsten carbide tool

Some of the properties of the tool are given below:

Table 4 Characteristics of Tungsten carbide tool

| S. No. | Properties | Values |
|---|---|---|
| 1 | Density, (D) | 15.5 Kg/$m^3$ |
| 2 | Melting point, (T) | 2880 $^oC$ |
| 3 | Thermal conductivity, (λ) | 110 W/m.K |
| 4 | Electrical resistivity, (ρ) | 0.2 μΩ.m |
| 5 | Elastic modulus, (E) | 630 GPa |
| 6 | Ultimate tensile strength, (UTS) | 344 MPa |
| 7 | Poisson's ratio, (ν) | 0.3 |
| 8 | Yield strength, (ε) | 140 MPa |
| 9 | Specific heat, (cp) | 184 J/Kg.$^oC$ |
| 10 | Rockwell hardness, (HR) | 91 HRC |

©IJRASET: All Rights are Reserved | SJ Impact Factor 7.538 | ISRA Journal Impact Factor 7.894 |

*2) High Carbon Steel Tool*

The table for the high steel carbon tool for the properties are given below:

Table 5 Chemical composition of High carbon steel tool

| Elements | Fe | S | P | Mn | C |
|---|---|---|---|---|---|
| Wt% | 98.56 | 0.05 | 0.04 | 0.41 | 98.56 |



Fig. 4 High Carbon Steel Tool

Above are given the picture we have taken for the high carbon steel tool which we have taken consideration for the working tool. Below are given the properties for high carbon steel tool

Table 6 Characteristics of High-speed steel tool

| S. No. | Properties | Values |
|---|---|---|
| 1 | Density, (D) | 7.85 Kg/m$^3$ |
| 2 | Melting point, (T) | 1515 $^o$C |
| 3 | Thermal conductivity, (λ) | 49.8 W/m.K |
| 4 | Electrical resistivity, (ρ) | 0.18 μΩ.m |
| 5 | Elastic modulus, (E) | 205 GPa |
| 6 | Ultimate tensile strength, (UTS) | 685 MPa |
| 7 | Poisson's ratio, (ν) | 0.29 |
| 8 | Yield strength, (ε) | 525 MPa |
| 9 | Specific heat, (cp) | 461 J/Kg.KA |
| 10 | Rockwell hardness, (HR) | 13 HRC |

*B. Work Piece*

Below are given the work piece we have picked up for the experimentation. We gave chosen two work pieces of same chemical properties for this; both are made up of titanium alloy.

The chemical and physical properties re given below:

Titanium alloy (Ti-6Al-4V)

Table 7 Chemical constituents of titanium alloy (Ti-6Al-4V)

| Elements | Al | V | Fe | O | C | N | Y | H | Ti |
|---|---|---|---|---|---|---|---|---|---|
| Wt% | 6.1 | 4 | 0.16 | 0.11 | 0.02 | 0.01 | 0.001 | 0.001 | 89.578 |

Chemical constitution is given below with details:



Fig. 5 Titanium alloy workpieces

Table 8 Characteristics of selected Titanium alloy

| S. No. | Properties | Values |
|---|---|---|
| 1 | Density, (D) | 4.428 Kg/m$^3$ |
| 2 | Melting point, (T) | 1660 $^o$C |
| 3 | Thermal conductivity, (λ) | 16.6 W/m.K |
| 4 | Electrical resistivity, (ρ) | 1.78 μΩ.m |
| 5 | Elastic modulus, (E) | 113 GPa |
| 6 | Ultimate tensile strength, (UTS) | 900 MPa |
| 7 | Poisson's ratio, (ν) | 0.33 |
| 8 | Yield strength, (ε) | 880 MPa |
| 9 | Specific heat, (cp) | 526.3 J/Kg.$^o$C |
| 10 | Rockwell hardness, (HR) | 36 HRC |

*C. Coolant*

The coolant is a very significant and important component of these kind of experiment. Because the tool is working against the workpieces and it produces heat thought friction. The heat produced in the process can do wear and tear of work pieces and also damage the work pieces or the tool. To prevent such damages a coolant is used to avoid these things. It also helps is gaining superb finish of the product.

The coolant taken in the experiment are palm oil and coconut oil. We have observed these two coolants for most of the studies.

*1) Palm Oil*

The chemical and physical properties of palm oil given below:

Table 9 Chemical composition of Palm Oil

| Elements | Saturated fatty acids | | | Monounsaturated fatty acid | Poly-natural fatty acid |
|---|---|---|---|---|---|
| | Palmitic Acid | Stearic acid | Myristic acid | Oleic acid | Linoleic acid |
| Wt% | 44 | 5 | 1 | 40 | 10 |

Table 10 Characteristics of Palm Oil

| S. No. | Properties | Values |
|---|---|---|
| 1 | Density, (D) | 0.947 g/ml |
| 2 | Heat absorbing capacity, (C) | 2.857 J/Kg.$^o$C |
| 3 | Thermal conductivity, (λ) | 0.156 W/m.K |
| 4 | Corrosion resistance | 98% |
| 5 | Specific heat, (cp) | 2.4 J/Kg.$^o$C |
| 6 | Economic value, (Rs.) | Low cost |
| 7 | Viscosity, (**η**) | 77.19 mPas |
| 8 | Harmful to operate and bearing | No |
| 9 | Fire point | 341 $^o$C |
| 10 | Melting point, (T) | 35.7 $^o$C |
| 11 | Smoke point | 223 $^o$C |

©IJRASET: All Rights are Reserved | SJ Impact Factor 7.538 | ISRA Journal Impact Factor 7.894 |

*2) Coconut Oil*

The physical and chemical properties of coconut oil is given below:

Table 11 Chemical composition of coconut oil

| Elements | Caprylic acid | Capric acid | Lauri c acid | Myristic acid | Palmitic acid | Stearic acid | Oleic acid | Linoleic acid |
|---|---|---|---|---|---|---|---|---|
| Wt% | 8 | 7 | 49 | 8 | 8 | 2 | 6 | 2 |

Table 12 Characteristics of coconut oil

| S. No. | Properties | Values |
|---|---|---|
| 1 | Density, (D) | 0.903 g/ml |
| 2 | Heat absorbing capacity, (C) | 2.1 J/Kg.$^{o}$C |
| 3 | Thermal conductivity, (λ) | 0.161 W/m.K |
| 4 | Corrosion resistance | 97% |
| 5 | Specific heat, (cp) | 2.2 J/Kg.$^{o}$C |
| 6 | Economic value, (Rs.) | Low cost |
| 7 | Viscosity, (**η**) | 39 mPas |
| 8 | Harmful to operate and bearing | No |
| 9 | Fire point | 329 $^{o}$C |
| 10 | Melting point, (T) | 24.8 $^{o}$C |
| 11 | Smoke point | 204 $^{o}$C |

*D. Machines And Equipment*

The machinery used for the following process in the experiment is CNC lathe. A CNC lathe is a piece of equipment that holds the material or part in place and rotates it using the main spindle while the cutting tool that works on the component is attached and moved on other axes. A basic CNC lathe runs on two dimensions, with the cutting tool set in place at 8 to 24 station turrets.

*1) Cnc Lathe Machine*

Details for the machines are given below:

Table 13 CNC lath machine details

| Brand | | HYTECH |
|---|---|---|
| Model | CLT 100 | |
| No. of axis | Two Dimensional axes (X, Z) | |

This HYTECH CNC trainer lathe machine was used to manufacture a work piece made of Titanium alloy (Ti-6Al-4V) with a highly polished surface.




Fig. 6 HYTECH CNC trainer lathe machine

The features of CNC machine used for the process are given below:

*a)* Industrial Slant–Bed Design
*b)* PC-based
*c)* Eight Station programmable Turret
*d)* Programmable Spindle
*e)* Fully enclosed working area
*f)* Pneumatic chuck
*g)* Auto door
*h)* Flexible Manufacturing System (FMS) Suitable
*i)* 100 to 3000 Spindle rpm

*2) Surface Roughness Tester*

A roughness tester is used to determine the surface texture or roughness of a material fast and precisely. In micrometres or microns (µm), a roughness tester displays the measured roughness depth (Rz) as well as the mean roughness value (Ra).




Fig. 7 Taylor Hobson surface roughness tester

Surtronic S-100 stylus surface roughness tester is a quick and dedicated equipment capable of measuring any height without any adjustment on any surface, even curved. Surtronic S-100 is a small, sturdy surface finish tester that offers a comprehensive set of recognisable measurement data, including a particular profile graph, in a matter of seconds after pressing the measurement button.

*3) Vernier Calipers*

The vernier caliper is one of the most commonly used measurement tools, second only to the measuring scale. The vernier calliper allows users to measure distances with much more precision. The vernier calliper measures an object's external and internal diameters, and the vernier scale is displayed on the vernier calliper.

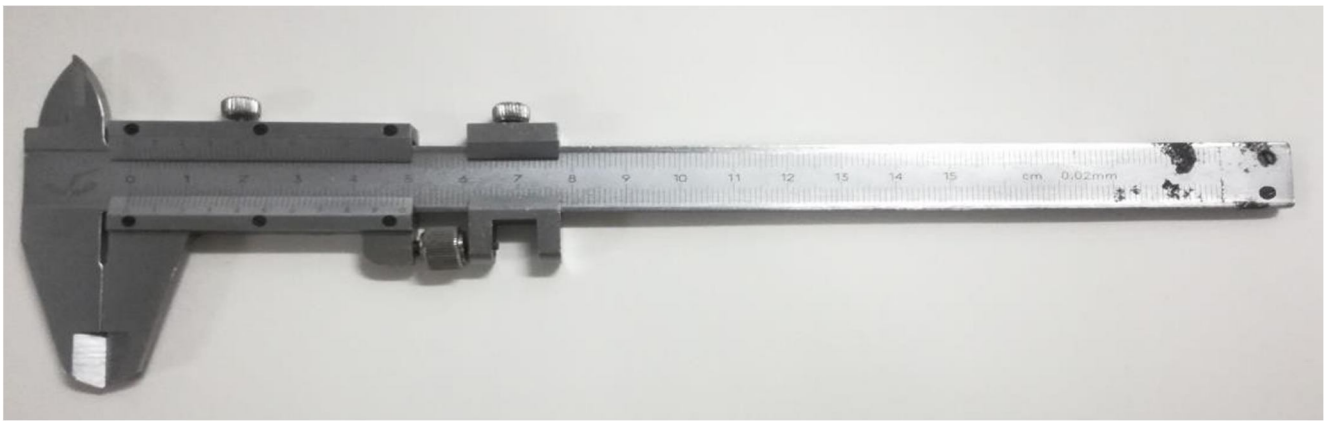


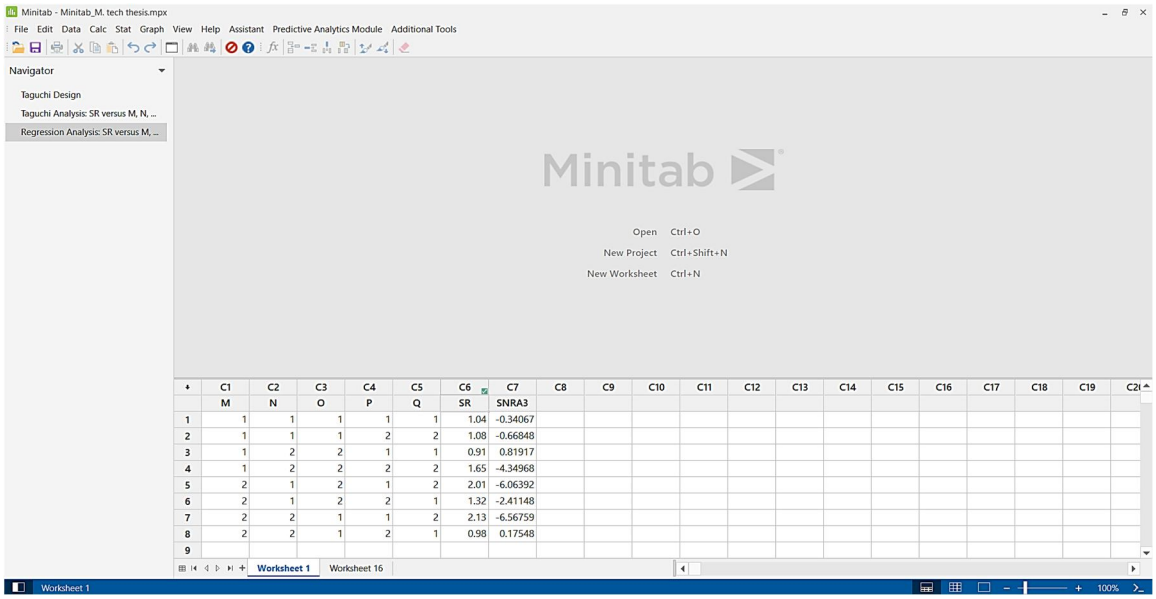

Fig. 9 Vernier Calipers

*4) Statistical Software (Minitab-19)*

Minitab Statistical Software can examine current and historical data to identify trends, identify and anticipate patterns, uncover hidden correlations between variables, and produce striking visualisations to address even the most difficult challenges and possibilities. It can discover, predict and achieve the visualisation of the data that can be through only to statistical ways.

We are using the statistical software to determine the optimal values from all the selected values of different components. To assess the consequence of the process parameters as feed, the percentage contribution of the corresponding parameters may be well resolved using Minitab - 19 software.

While the Taguchi method may govern and judge the consequence of the relevant factors on the entire process, the rate, depth of cut, cutting speed, tool material, and MQL lubrication cannot. Minitab -19 software was used to prepare the experimental design array and to evaluate all of the results using statistical techniques.




| | C1 | C2 | C3 | C4 | C5 | C6 | C7 |
|---|---|---|---|---|---|---|---|
| | M | N | O | P | Q | SR | SNRA3 |
| 1 | 1 | 1 | 1 | 1 | 1 | 1.04 | -0.34067 |
| 2 | 1 | 1 | 1 | 2 | 2 | 1.08 | -0.66848 |
| 3 | 1 | 2 | 2 | 1 | 1 | 0.91 | 0.81917 |
| 4 | 1 | 2 | 2 | 2 | 2 | 1.65 | -4.34968 |
| 5 | 2 | 1 | 2 | 1 | 2 | 2.01 | -6.06392 |
| 6 | 2 | 1 | 2 | 2 | 1 | 1.32 | -2.41148 |
| 7 | 2 | 2 | 1 | 1 | 2 | 2.13 | -6.56759 |
| 8 | 2 | 2 | 1 | 2 | 1 | 0.98 | 0.17548 |
| 9 | | | | | | | |

Fig. 8 Design expert software Minitab-19

## V. EXPERIMENT DETAILS

In this exploration the pace of feed, cut profundity, speed of cutting, apparatus material and MQL oil mode (sorts of coolants) are five boundaries were recognized. After the primer tests, the scopes of the different boundaries and the most extreme cutting not entirely settled. To research the non-linearity result of the cycle boundaries, all boundaries were learned at two levels.

For every influencing parameter we considered two most observing factors that are taken for most of the experiments in studies. We considered it with two levels of parameters, to apply Taguchi Design for our experiment. All the considered factors with two levels are given in the table 14.

Table 14 Control factors and levels

| Control Factors | Levels | |
|---|---|---|
| | 1 | 2 |
| Feed rate (M), mm/rev. | 0.1 | 0.2 |
| Depth of cut (N), mm | 0.1 | 0.15 |
| Cutting speed (O), rev/min | 2000 | 2500 |
| Tool material (P) | WC | HCS |
| Lubricating mode (Q) | Palm Oil | Coconut Oil |

Two titanium alloy bars with a diameter of 20 mm (Fig. 5) are shown of Grade 5. (Ti- 6Al-4V) were used as work material. Table 8 shows the chemical constituents of the work material. The work content is a grade 5 (+).

The Titanium alloy work pieces were machined using a tungsten carbide and high carbon steel inserted tool with tool holder (Fig 9 and 10); images of the tungsten carbide and high carbon steel inserted tools are provided in Figures 4 and 5, respectively.



Fig. 9 Tungsten carbide tool with tool holder

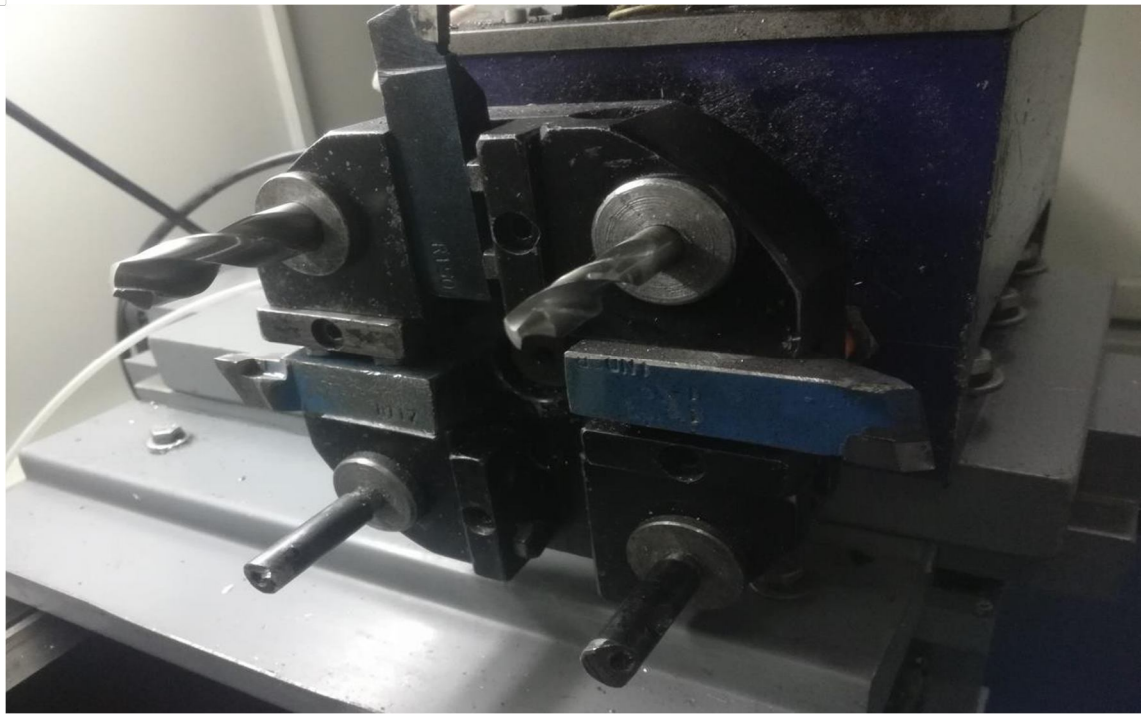


Fig. 10 High carbon steel tool with tool holder

According to Taguchi quality design theory, a conventional L8 orthogonal array (OA) was chosen for five factors and two levels, as shown in Table 14. The turning difficulties on the 'HYTECH CNC trainer lathe' were performed utilising a machine with the highest feasible spindle velocity of 3000 rpm and a spindle power of 2 HP, according to OA. Two distinct types of coolant are employed to regulate the temperature across the cutting for optimum surface finish. Fig. 11 and 12 shows the depict machining operations with tungsten carbide and high carbon steel tools in both lubricants (palm oil and coconut oil).

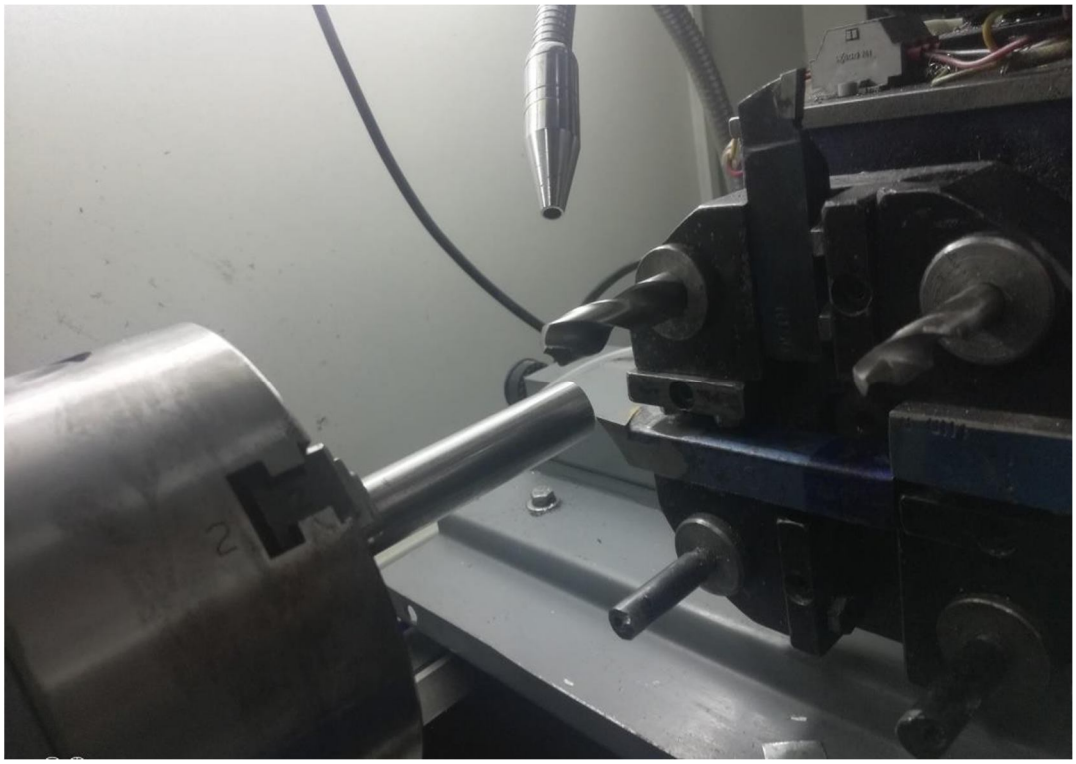


Fig. 11 Machining operation with tungsten carbide tool at both lubricant

©IJRASET: All Rights are Reserved | SJ Impact Factor 7.538 | ISRA Journal Impact Factor 7.894 |

Below are the given table formed in the Mini tab for applying the L8 orthogonal array. We make all the factors with two levels for applying Taguchi design.

Fig. 12 Machining operation with high carbon steel tool at both lubricant

Table 15 Control factors arrangements as per L8 orthogonal array, the considered outcomes and the correlated signal to noise ratios

| Trail No. | M | N | O | P | Q | Surface roughness (R), µm |
|---|---|---|---|---|---|---|
| 1 | 1 | 1 | 1 | 1 | 1 | 1.04 |
| 2 | 1 | 1 | 1 | 2 | 2 | 1.08 |
| 3 | 1 | 2 | 2 | 1 | 1 | 0.91 |
| 4 | 1 | 2 | 2 | 2 | 2 | 1.65 |
| 5 | 2 | 1 | 2 | 1 | 2 | 2.01 |
| 6 | 2 | 1 | 2 | 2 | 1 | 1.32 |
| 7 | 2 | 2 | 1 | 1 | 2 | 2.13 |
| 8 | 2 | 2 | 1 | 2 | 1 | 0.98 |

The MQL lubrication mode is used in this study. In the MQL lubrication method, vegetable oil-based cutting fluids such as Palm oil with a density of 0.497 g/ml and a viscosity of 77.19 mPas at 25°C and Coconut oil with a density of 0.9.3 g/ml and a viscosity of 39 mPas at 25°C are used as lubricants. These lubricants (Palm oil and Coconut oil) are free of chlorine, phenol, and other contaminants.

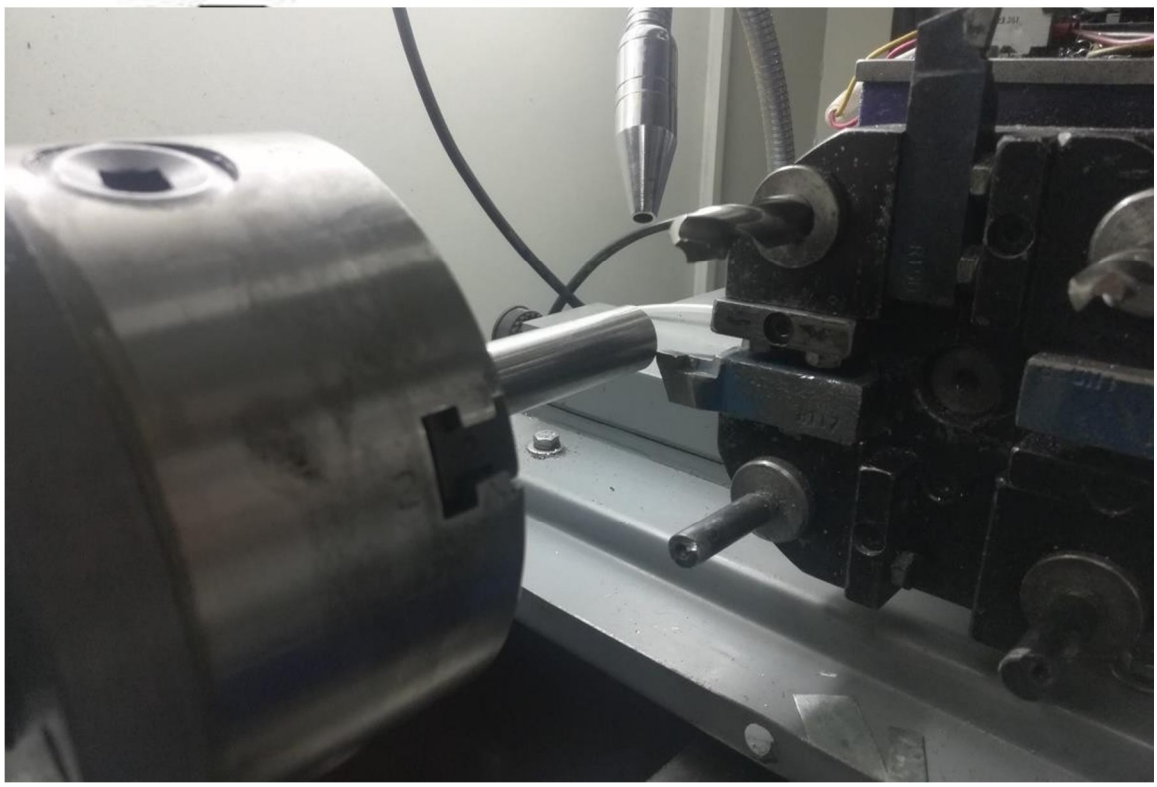


Fig. 13 MQL setup used in experiment

The tests in MQL-style approaches were guided by a narrow-pulsed jet nozzle and governed by an unstable speed control mechanism. Fig. 13 depicts the MQL configuration used in this study. It has a two-litre reservoir and a pneumatic piston pump for injecting coolant. A filtering regulator is installed in the airline to govern the air utilised in the MQL arrangement, and a coolant oil filter is also installed as an air breather to filter coolant oil to 139 microns.

A tension control button is used to guarantee that the fundamental pneumatic stress is conveyed to the arrangement. For the pneumatic cylinder siphon to work, an air controller and a solenoid valve are utilized to control the gaseous tension.

To deal with the recurrence of coolant oil cylinder siphon, electronic convertible clock is applied with as far as possible from 0.6 seconds to an hour (8 units). The pace of absolved from the siphon is 0.40 cc/stroke. To get the required absolved, the time of stroke and the delay between two strokes. At the machining focus shaft, a conveyable installation is fitted to the spout. The infusion spout could be situated anyplace on account of the adaptable plan during the machining system without impeding the workpiece or device. The release pressure is set at 4 kgf/cm$^2$, and the spout hole width is 1 mm.

Table 16 Taguchi design summary

| Design Summary | |
|---|---|
| Taguchi Array | L8(2^5) |
| Factors: | 5 |
| Runs: | 8 |
| Columns of L8(2^7) array: 1 2 3 4 5 | |

Above is the design summary for the Taguchi Design. We have as per decide the L8 two level with 5 parameters designs.

The operating coolant flood nozzle in a MQL configuration is oriented opposite to the feed direction. A simple surface roughness tester TAYLOR HOBSON Surtronic S-100 with a 15 mm cut off length was utilised to measure the machined surface. As the surface roughness in this study, an arithmetic mean average surface roughness (Ra) is used. Table 15 articulates the calculated amount of surface roughness. All trails were repeated twice, and the investigation was conducted using a mean reading.

## VI. RESULT AND DISCUSSION

Surface roughness reduction is the main objective of ANOM and ANOVA in this work. Therefore, for surface roughness, the "smaller the better kind" category has been selected. The S/N ratio in regard to the objective functions for each OA trial is supplied by:

From the table 2, we have taken the (smaller the better kind) category in Taguchi design.

| | |
|---|---|
| Smaller – the better | $-10 \times \log 10\ (sum\ (Y^2/n)$ |

Equations from the designs were used to resolve the associated S/N ratios for all tests of the L8 orthogonal array, and the results are provided in Table 15, which lists the parameter levels and combinations for the investigative machining parameters used in the L8 orthogonal array (OA).

In table 16, the Taguchi design summary is given for the L8 orthogonal array.

Table 17 Control factors in design with L8 orthogonal array with the S/N ratio outcome

| Trail No. | M | N | O | P | Q | SR | S/N RA3 |
|---|---|---|---|---|---|---|---|
| 1 | 1 | 1 | 1 | 1 | 1 | 1.04 | -0.34067 |
| 2 | 1 | 1 | 1 | 2 | 2 | 1.08 | -0.66848 |
| 3 | 1 | 2 | 2 | 1 | 1 | 0.91 | 0.81917 |
| 4 | 1 | 2 | 2 | 2 | 2 | 1.65 | -4.34968 |
| 5 | 2 | 1 | 2 | 1 | 2 | 2.01 | -6.06392 |
| 6 | 2 | 1 | 2 | 2 | 1 | 1.32 | -2.41148 |
| 7 | 2 | 2 | 1 | 1 | 2 | 2.13 | -6.56759 |
| 8 | 2 | 2 | 1 | 2 | 1 | 0.98 | 0.17548 |

©IJRASET: All Rights are Reserved | SJ Impact Factor 7.538 | ISRA Journal Impact Factor 7.894 |

Above given table are paste from the Minitab after the design experiment conducted for Taguchi.

Table 18 Response table for S/N ration and Means

| Response Table for Signal to Noise Ratios | | | | | |
|---|---|---|---|---|---|
| Smaller is better | | | | | |
| Level | M | N | O | P | Q |
| 1 | -1.1349 | -2.3711 | -1.8503 | -3.0383 | -0.439 |
| 2 | -3.7169 | -2.4807 | -3.0015 | -1.8135 | -4.4124 |
| Delta | 2.5820 | 0.1095 | 1.1512 | 1.2247 | 3.9730 |
| Rank | 2 | 5 | 4 | 3 | 1 |

| Response Table for Means | | | | | |
|---|---|---|---|---|---|
| Level | M | N | O | P | Q |
| 1 | 1.170 | 1.363 | 1.308 | 1.522 | 1.063 |
| 2 | 1.610 | 1.417 | 1.473 | 1.257 | 1.718 |
| Delta | 0.440 | 0.055 | 0.165 | 0.265 | 0.655 |
| Rank | 2 | 5 | 4 | 3 | 1 |

The optimal numbers of control parameters were determined using the analysis of means (ANOM) in accordance with the S/N ratio; the results of ANOM for surface roughness are shown in below figures. The superior combination level is the S/N ratio of a parameter at its highest value. The data means plot of S/N ratio and the for the means are plotted in the Minitab, which are shown below.

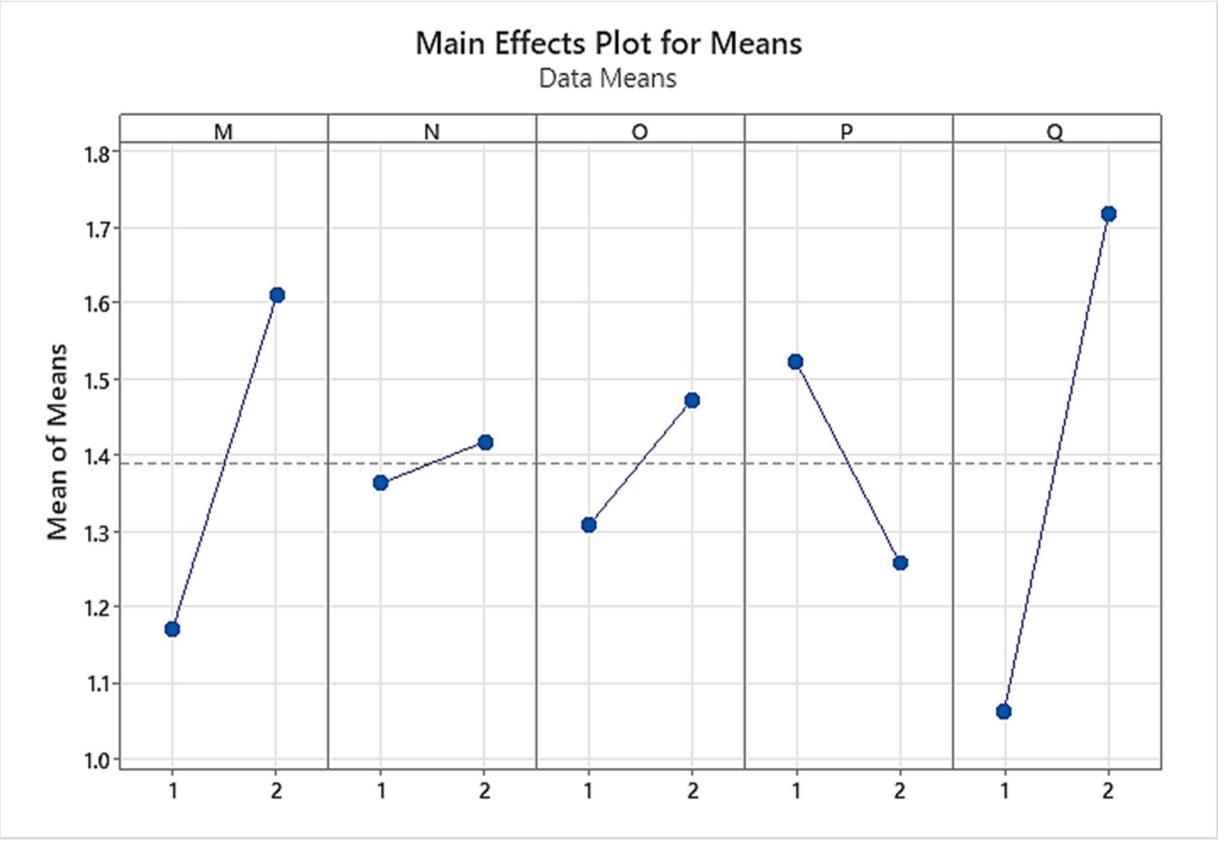



Fig. 14 Data Means main effect plot for Means

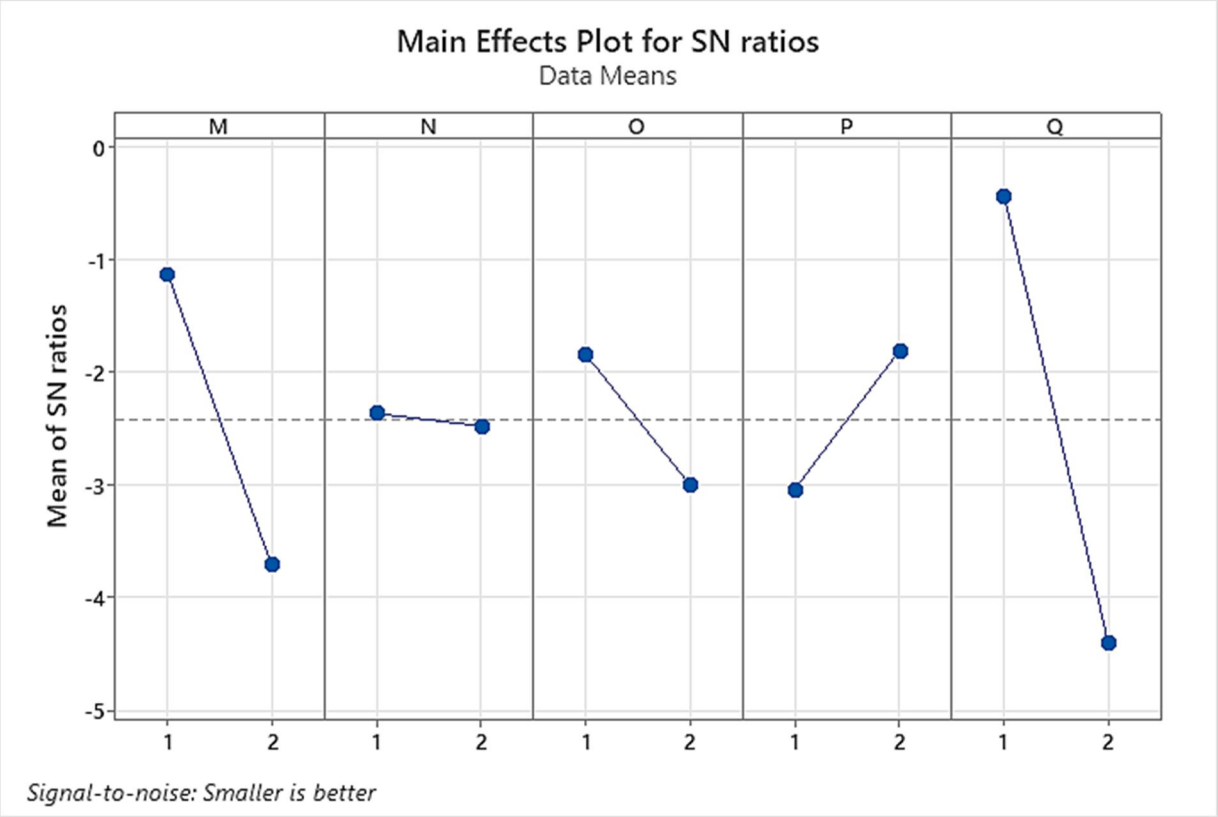



Fig. 15 Data Means Min effect plot for SN ratios

Lowest feed rate of 0.1 mm/rev (M1), lowest cut depth of 0.15 mm (N2), highest cutting speed of 2500 rpm (O2), tool material WC (P1), and MQL lubricating mode such as palm oil (Q1) are created as the optimal parameter configuration for the smoothest surface. The analysis of variance (ANOVA) has proven successful in allowing for a quantitative examination of the effects of control factors, as indicated by the S/N ratio.

By separating the total S/N ratio instability, which is computed as the sum of the squared deviations from the S/N ratio's absolute average multiplied by all errors and factors, the ANOVA analysis is carried out. A representation of the surface roughness results is shown in Table 18.

The MQL lubricating mode, including palm oil (52.91%) and feed rate (23.88%), has substantial contributions, according to the ANOVA, whereas the tool has a smaller impact.

The amount of material (8.66%) is significant in lowering surface roughness. On the other hand, a fast-cutting speed (3.36%) and a shallow cut (0.37%) had the least effect on reducing the roughness of the surface.

After the Taguchi method for the contribution effect of each parameter is to be determine from regression method. Regression is mainly a method which results in showing the contribution of each parameter taken for the experiment. It also gives us the equation for further usage. So that we do not have to do the experiment again and again. The equation can be used for validation of the model, or can be used for later use for new designs if the parameters are given to be same.

Below given are the model summary with each parameter contribution. The regression is applied with the 95 % Confidence Interval.

Table 19 Model summary

| S | R-sq | PRESS | R-sq(pred) | AICc | BIC |
|---|---|---|---|---|---|
| 0.296142 | 89.18% | 2.8064 | 0.00% | * | 6.70 |

©IJRASET: All Rights are Reserved | SJ Impact Factor 7.538 | ISRA Journal Impact Factor 7.894 |

Table 20 Analysis of Variance

| Analysis of Variance | | | | | | |
|---|---|---|---|---|---|---|
| Source | DF | Seq SS | Contribution | Adj SS | Adj MS | F-Value |
| Regression | 5 | 1.44620 | 89.18% | 1.44620 | 0.289240 | 3.30 |
| M | 1 | 0.38720 | 23.88% | 0.38720 | 0.387200 | 4.42 |
| N | 1 | 0.00605 | 0.37% | 0.00605 | 0.006050 | 0.07 |
| O | 1 | 0.05445 | 3.36% | 0.05445 | 0.054450 | 0.62 |
| P | 1 | 0.14045 | 8.66% | 0.14045 | 0.140450 | 1.60 |
| Q | 1 | 0.85805 | 52.91% | 0.85805 | 0.858050 | 9.78 |
| Error | 2 | 0.17540 | 10.82% | 0.17540 | 0.087700 | |
| Total | 7 | 1.62160 | 100.00% | | | |

The Durbin-Watson Statistical number comes to be 2.479, which is good fit for the statistical analysis point of view. The $R^2$ is also comes to be 0.89, which means 89.18 % of the data is “goodness of fit” for the observations we take for experiment.
The validation tests were finished using the optimal control level settings, and the assessment inaccuracy was declared to be inside the 95% confidence interval, proving the viability of the proposed surface roughness model. Table 21 lists the ideal values that correspond to the top pairs of control parameters for lowering surface roughness.
Below is the given regression equation we got form the Minitab.
Regression Equation

SR = - 0.185 + 0.440 M + 0.055 N + 0.165 O - 0.265 P + 0 .655 Q

The given equation we have for later use in the field. In this M, N, O, P, Q are the given parameters for the experiment.




Fig. 16 Workpiece of titanium alloy (Ti-6Al-4V) after tuning

The major effect plots (Fig. 14 and 15) are produced by using MINITAB statistical software to select the effects of control parameters on the surface roughness. Figure 16 depicts the titanium composite material workpiece (Ti-6Al-4V) following turning, at which point the surface's roughness was assessed.

©IJRASET: All Rights are Reserved 

*A. Analysis Of Surface Roughness*

1) *Effect Of Feed Rate:* ANOVA clearly demonstrates that the rate of feed is involved (23.88 percent) in reducing the surface roughness (Table 13). In general, as feed rate increases for MQL lubrication with palm oil, the surface roughness increases. However, with different feed rates compared to coconut oil, palm oil exhibits a decrease in surface roughness as a result of the MQL delivery pressure, which clears chips (debris) from the cutting point.As the feed rate increases, there is less time to remove the heat from the cutting zone, which increases surface roughness. There is also a large rate of material removal and an accumulation of chips between the work piece and the tool tip, as shown in Fig. 15.
2) *Impact Of Depth Of Cut: The cut depth clearly contributes (0.37 percent) to the decrease in surface roughness, as shown by ANOVA (Table 13). Surface roughness decreases with deeper cuts, primarily because of the machine tool's increased vibration and thermal stress. which Fig. 15 is quite evident. In addition, there is significant tool wear and high friction because there is a lot of surface contact between the tool and the workpiece.*
3) *Impact Of Cutting Speed:* According to an ANOVA analysis, the speed of cutting contributes 3.36 percent to reducing surface roughness (Table 13). Figure 18 shows that with increased cutting speed, the surface roughness of the machined segment decreased. This is because increasing the softness of the work piece material reduces the forces of cutting, leading to a superior surface finish; maximum spindle speed is proportional to the temperature of cutting at the highest level. Additionally, the chip will separate at the highest spindle speed with the least amount of material deformation at the tool tip, continuing to preserve the characteristics of the machined surface and aiming for the lowest possible level of surface roughness. The roughness can be enhancing with the increase of cutting speed. However, with the speed like 2000-2500 rpm the enhancement is very linear by the time the speed increase. By increasing cutting speed, BUE is reduced, and as a result, the surface finish is improved. As a result of less significant lateral plastic flow, the surface roughness can be improved. Increasing cutting speed decreases the material's plasticity, which causes a lower increase in the peak-to-valley height of the machined surface finish. Additionally, at low cutting speeds, grooves develop on the tool wear face. The importance of the surface roughness reduction increases with the growth of the grooves.

Table 21 Optimal Control factor arrangement and the correlated optimal values of surface roughness

| Response | Optimal process parameter setting | | | | | Optimal value |
|---|---|---|---|---|---|---|
| | Feed rate (mm/rev.) | Depth of cut (mm) | Cutting speed (rpm) | Tool material | Lubricating mode | |
| Surface roughness | 0.1 | 0.15 | 2500 | WC | Palm Oil | 0.91 |

4) *Effect of Tool Material:* The quality of the workpiece or component is significantly influenced by the surface finish of the component or workpiece. It can be seen from ANOVA (Table 20) that does help to lessen the roughness of the titanium alloy's surface (8.66 %). Due to the greater chemical reactivity and hardness of titanium alloy and resulting change in tool geometry, titanium has a propensity for galling when used in cutting tools. Due to the titanium alloy's reduced thermal conductivity, the HCS tool has a relatively short lifetime when used for high-speed cutting and can only be used at the lowest possible cutting speed.
5) *Impact of Lubricating Mode:* It is evident that the MQL lubrication with palm oil significantly reduces the surface roughness as indicated by the ANOVA analysis, contributing 52.91 percent of the total reduction. When used in MQL machining, palm oil effectively provides lubrication, cooling, and evaporative as well as convective heat transfer. In contrast to conditions using coconut oil as lubricant, Fig. 15 shows that MQL machining using palm oil has demonstrated effectiveness in reducing surface roughness. Therefore, it is advised that MQL machining be done using palm oil to improve surface polish, lower cost, use less lubricant, and lessen pollution.

## VII. CONCLUSION

Under various cutting circumstances, the surface roughness of titanium machining alloys (Ti-6Al-4V) has been investigated during the turning process. In this paper, the Taguchi method of optimization is described for titanium alloy machining with tungsten carbide and high carbon steel tools in order to be able to minimise the roughness of the surface. The following conclusions are drawn from an analysis of the experiment's results:

1) When turning titanium alloy, a combination of low feed rate, strong cut depth, strong cutting speed, tungsten carbide tool, and MQL lubricating with palm oil produces the least rough surface.
2) The surface roughness caused by the machining parameters has been identified, and by using the Taguchi approach, the best machining conditions will be adhered to in order to lessen the surface roughness.
3) According to the findings of the analysis of variance, titanium alloy turning procedures might significantly reduce surface roughness by using the indicated machining settings:

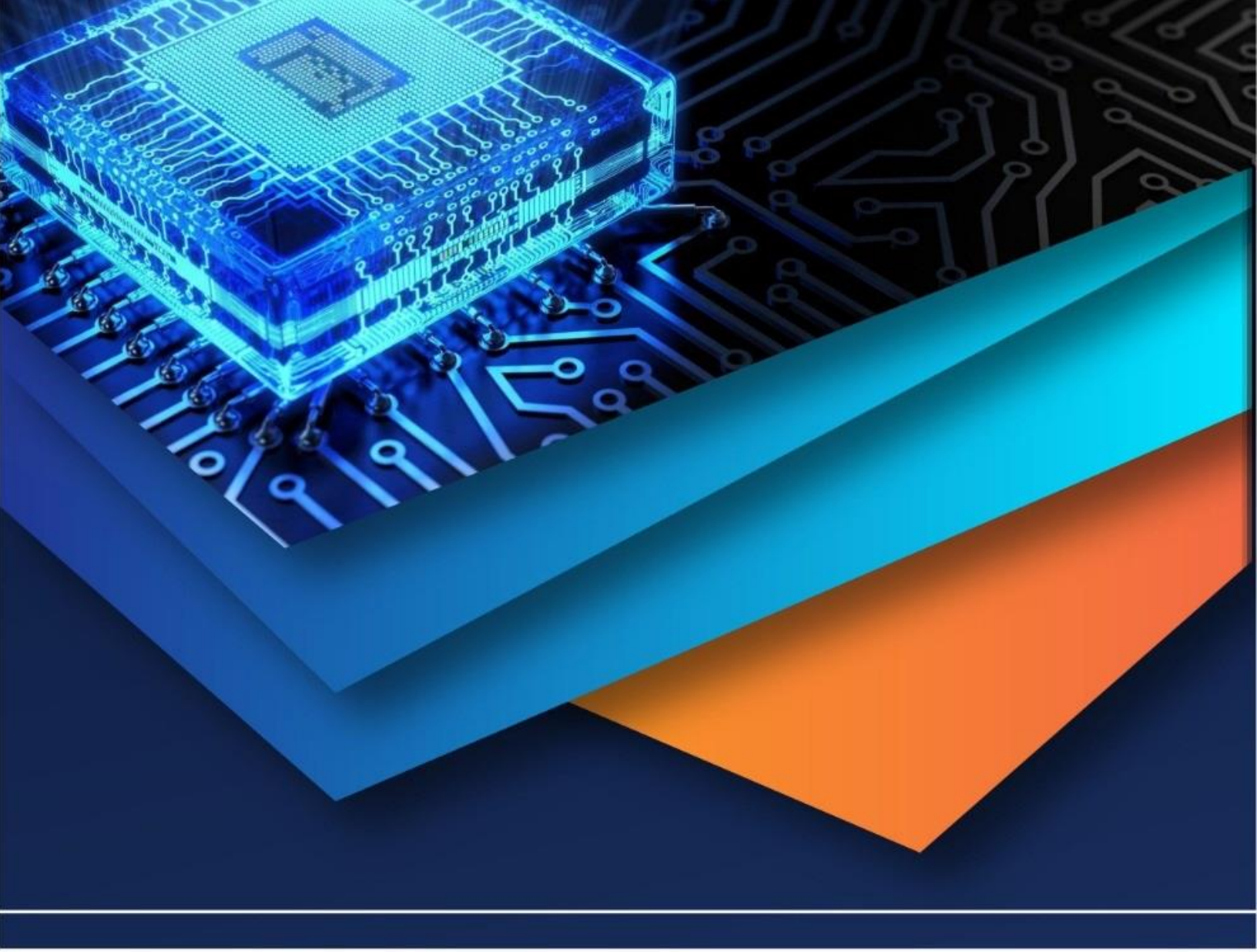
| Parameter | Value used |
|---|---|
| Rate of feed | 0.1 mm/rev. |
| Cut-depth | 0.15 mm |
| Rate of cutting | 2500 rpm |
| Tool | Tungsten Carbide tool |
| Oil used | Palm Oil |

4) Lubricating with palm oil (52.91 percent) and feeding at a higher pace (23.88 percent) both significantly reduce surface roughness. The tool material has a vital role in smoothing down the surface as well.
5) When machining MQL using palm oil as opposed to coconut oil, the surface roughness is minimised.
6) The roughness of the surface rose as the rate of feed decreased, whereas it decreased as the cutting speed increased.
7) To get a superior surface finish when cutting titanium composite material (Ti-6Al-4V), WC insert was used as the cutting tool material.

## REFERENCES

[1] M. Rahaman, Y. Wong, and A. rahamath Zareena, “Machinability of Titanium Alloys,” JSME, 2002, Accessed: Jul. 23, 2022. [Online]. Available: https://www.jstage.jst.go.jp/article/jsmec/46/1/46_1_107/_pdf/-char/en
[2] P. J. Arrazola, A. Garay, L. M. Iriarte, M. Armendia, S. Marya, and F. le Maitre, “Machinability of titanium alloys (Ti6Al4V and Ti555.3),” journal of materials processing technology, 2009, Accessed: Jul. 23, 2022. [Online]. Available: https://pdf.sciencedirectassets.com/271356/1-s2.0-S0924013609X00038/1-s2.0-S0924013608004998/main.pdf
[3] C. Castellani et al., “Bone-implant interface strength and osseointegration: Biodegradable magnesium alloy versus standard titanium control,” Acta Biomater, vol. 7, no. 1, pp. 432–440, 2011, doi: 10.1016/J.ACTBIO.2010.08.020.
[4] X. Liu, P. K. Chu, and C. Ding, “Surface modification of titanium, titanium alloys, and related materials for biomedical applications,” 2005, doi: 10.1016/j.mser.2004.11.001.
[5] P. M. Faris, M. A. Ritter, K. E. Davis, and H. M. Priscu, “Ten-Year Outcome Comparison of the Anatomical Graduated Component and Vanguard Total Knee Arthroplasty Systems,” The Journal of Arthroplasty, vol. 30, no. 10, pp. 1733–1735, Oct. 2015, doi: 10.1016/J.ARTH.2015.04.042.
[6] W. Becker, P. Hujoel, B. E. Becker, and P. Wohrle, “Dental Implants in an Aged Population: Evaluation of Periodontal Health, Bone Loss, Implant Survival, and Quality of Life,” Clin Implant Dent Relat Res, vol. 18, no. 3, pp. 473–479, Jun. 2016, doi: 10.1111/CID.12340.
[7] S. Karmarker, W. Yu, and H. M. Kyung, “Effect of surface anodization on stability of orthodontic microimplant,” Korean J Orthod, vol. 42, no. 1, pp. 4–10, Feb. 2012, doi: 10.4041/KJOD.2012.42.1.4.
[8] H. Ao et al., “Improved hMSC functions on titanium coatings by type I collagen immobilization,” J Biomed Mater Res A, vol. 102, no. 1, pp. 204–214, 2014, doi: 10.1002/JBM.A.34682.
[9] S. Mei et al., “Antibacterial effects and biocompatibility of titanium surfaces with graded silver incorporation in titania nanotubes,” Biomaterials, vol. 35, no. 14, pp. 4255–4265, May 2014, doi: 10.1016/J.BIOMATERIALS.2014.02.005.
[10] G. Jin et al., “Synergistic effects of dual Zn/Ag ion implantation in osteogenic activity and antibacterial ability of titanium,” Biomaterials, vol. 35, no. 27, pp. 7699–7713, Sep. 2014, doi: 10.1016/J.BIOMATERIALS.2014.05.074.
[11] “(PDF) Titanium in Medicine | sankeerth julapally - Academia.edu.” https://www.academia.edu/35029184/Titanium_in_Medicine (accessed Jul. 23, 2022).
[12] B. H. Hanson, “Present and future uses of titanium in engineering,” Materials & Design, vol. 7, no. 6, pp. 301–307, Nov. 1986, doi: 10.1016/0261-3069(86)90099-3.
[13] H. Hassanpour, M. H. Sadeghi, H. Rezaei, and A. Rasti, “Experimental Study of Cutting Force, Microhardness, Surface Roughness, and Burr Size on Micromilling of Ti6Al4V in Minimum Quantity Lubrication,” Materials and Manufacturing Processes, vol. 31, no. 13, pp. 1654–1662, Oct. 2016, doi: 10.1080/10426914.2015.1117629.
[14] C.Bandapalli, K. K. Singh, B. M. Sutaria, and D. V. Bhatt, “Experimental investigation of top burr formation in high-speed micro-end milling of titanium alloy,” https://doi.org/10.1080/10910344.2018.1449213, vol. 22, no. 6, pp. 989–1011, Nov. 2018, doi: 10.1080/10910344.2018.1449213.
[15] C. Bandapalli, B. M. Sutaria, and D. V. P. Bhatt, “The Comparison of Cutting Tools for High-Speed Machining of Ti-6Al-4V ELI Alloy (Grade 23),” Titanium Alloys - Novel Aspects of Their Processing [Working Title], Nov. 2018, doi: 10.5772/INTECHOPEN.80641.

©IJRASET: All Rights are Reserved | SJ Impact Factor 7.538 | ISRA Journal Impact Factor 7.894 |



10.22214/IJRASET

45.98

IMPACT FACTOR: 7.129

IMPACT FACTOR: 7.429

# INTERNATIONAL JOURNAL FOR RESEARCH

IN APPLIED SCIENCE & ENGINEERING TECHNOLOGY

Call : 08813907089 (24*7 Support on Whatsapp)